GEOPHYSICS, VOL. 66, NO. 1 (MAY-JUNE 2001); P. 824–835, 17 FIGS.

Cross-borehole delineation of a conductive ore deposit in a resistive host—experimental design

David Johnson*, Elena Cherkaev‡, Cynthia Furse**, and Alan C. Tripp§

ABSTRACT

The finite-difference time-domain method is used for high-resolution full-wave analysis of cross-borehole electromagnetic surveys of buried nickel sulfide deposits. The method is validated against analytical methods for simple cases, but is shown to be a valuable tool for analysis of complicated geological structures such as faulted or layered regions. The magnetic fields generated by a wire loop in a borehole near a nickel sulfide deposit are presented for several cases. The full-wave solution is obtained up to 200 MHz, where quasi-static methods would have failed. The dielectric response is included in the solution, and the diffractive nature of the field is observed. The sensitivity of each receiver in a vertical line in the cross borehole is presented and analyzed to provide an optimal weighting for receivers that can be applied to an experimental study.

INTRODUCTION

An important class of mineral deposits has highly conductive ore zones embedded in a resistive host. Examples include the Kambalda (Gresham and Loftus-Hills, 1981), Sudbury basin (Stanton, 1972), and Voisey Bay nickel deposits, where the ore bodies are dominated by highly conductive pyrrhotite, giving ore conductivities of about 10^5–10^6 S/m. Cross-bore electromagnetic (EM) surveys are desirable in delineating such deposits. In particular, source fields with excitation frequencies in the megahertz range have been suggested by numerous authors to be of particular usefulness in resolving the geometry of such features (Rao and Rao, 1983; Stolarczyk et al., 1988; Nickel and Cerny, 1989; Stolarczyk, 1990, 1992; Thomson et al., 1992; Wedepohl, 1993; Fullagar and Livelybrooks, 1994; Pitt and Kramers, 1996). Although designing and interpreting an experiment at these frequencies has been difficult given the lack of appropriate modeling software, recent advances in modeling (Johnson, 1997; Johnson et al., 1998) can be used to facilitate experimental design. The purpose of this paper is to illustrate the state of the art in experiment design in the megahertz range using finite-difference time-domain (FDTD) modeling software.

ALGORITHMS AVAILABLE FOR MODELING

The geophysical models discussed in this paper consist of highly conductive massive sulfide bodies situated within a weakly conducting host rock. In this case, the electromagnetic fields attenuate very rapidly within the conductor. For instance, if we consider electromagnetic fields with a frequency of 1 MHz incident upon sulfide mineralization (e.g., massive pyrrhotite) of conductivity 10^4 S/m, then the skin depth within the conductor will be 5 mm. For fields outside of the orebody, we can model the orebody as a perfect electric conductor (PEC), where we assume that the fields vanish within the object.

Several existing algorithms can be considered for this modeling problem. Annan (1974) presented a numerical approximation for the response of a perfectly conducting plate in free space. This approximation, although useful, has a limited accuracy for conducting host media. Moreover, the thin plate model is lacking in geometric flexibility. Volume current integral equation codes, which permit simulation of a conducting host, become numerically cumbersome or unstable for high target conductivities or target-host conductivity contrasts (Hohmann, 1983; San Filipo et al., 1985). In addition, neglecting displacement currents may not be justifiable for the electrical properties and transmitter frequencies of interest. These considerations narrow the field of candidates for codes with which to perform this modeling.

Published on Geophysics Online October 25, 2000. Manuscript received by the Editor January 11, 1999; revised manuscript received August 29, 2000.
*Rio Tinto Exploration, 2 Kilroe Street, Milton, Queensland, 4064, Australia. E-mail: David.Johnson@exl.riotinto.com.au.
‡University of Utah, Department of Mathematics, 233 JWB, Salt Lake City, Utah 84112.
**Utah State University, Department of Electrical and Computer Engineering, UMC 4120, Logan, Utah 84322-4120. E-mail: furse@ece.usu.edu.
§University of Utah, Department of Geology and Geophysics, 717 WBB, Salt Lake City, Utah, 84112.

Four modeling codes were initially identified for experimentation and possible customization to the geophysical case at hand.

Wang-Hohmann (WH) code

A code described by Wang and Hohmann (1993) was developed for the quasistatic diffusion regime. It uses a modified version of the Du Fort–Frankel method to step Maxwell's equations in time on a Yee staggered grid. A homogeneous Dirichlet boundary condition is imposed on the fields at the subsurface boundaries of the computational mesh to truncate the computational domain. The mesh boundaries are placed a sufficient distance from the region of interest to ensure that outward propagating electromagnetic fields attenuate sufficiently before reaching these perfectly reflecting surfaces. Expansion of the mesh beyond the region of interest is performed using gradually increasing cell dimensions, which is feasible in the diffusive regime because field variations become smoother with increasing distance from transmitters and scatterers. This code is appropriate for calculating the responses for the lower excitation frequency content used in the original Wang-Hohmann study, but would not be valid for the present case of interest in the megahertz range because the quasi-static approximation would not be valid

Furse-Johnson (FJ) code

A code written by Cynthia Furse and others in the Department of Electrical Engineering, University of Utah, is an implementation of the Yee (1966) method using second-order accurate central difference approximations for the temporal and spatial derivatives in Maxwell's equations (Furse et al., 1990). This uses the standard FDTD method. Derivation of the time-stepping equations is discussed in several texts (e.g., Taflove and Umashankar, 1989). Both electric conduction and displacement currents are included in the model. This code was originally developed for models contained within a region of free space, and used Mur (1981) second-order absorbing boundary conditions (ABC) on the mesh boundaries. This ABC is inappropriate for simulating broadband EM responses of targets in dispersive media because it is based upon an equation in which phase velocity is assumed constant. An accurate ABC for lossy host materials is required. Attention has recently been focussed on perfectly matched layer (PML) absorbing boundary conditions, which reportedly lead to superior accuracy (Berenger, 1994; Chew and Weedon, 1994; Chen et al., 1996). Differing formulations of the PML for lossy media have been published by Berenger (1994), Fang and Wu (1995), Chen et al. (1996), and others. The Chen et al. formulation was chosen for its ease of implementation.

Wang-Tripp (WT) code

A third code, described by Wang and Tripp (1996), is another full-field numerical solution to Maxwell's equations, incorporating both electric conduction and displacement currents. The code differs from the conventional Yee algorithm in two ways. First, the spatial derivatives are approximated by special optimized second-order divided differences, which lead to better numerical dispersion characteristics. In addition, the computational mesh is terminated using Liao absorbing boundary conditions, which are described by Chew (1990). A major disadvantage of this boundary condition is the requirement that transmitters, scatterers, and receivers be placed a large distance from the mesh boundaries, so the region of interest must be padded with extra cells (Wang and Tripp, 1996). In contrast, PML absorbing boundary conditions have been shown to perform well in cases where the transmitter is placed close to the mesh boundary (Chen et al., 1996). An optimal solution for future work might be to incorporate PML absorbing boundary conditions into the optimized second-order finite difference scheme described by Wang and Tripp (1996).

In these three modeling codes, the boundary condition

$$\mathbf{E}_{tan} = 0 \tag{1}$$

was imposed on the tangential electrical fields at the surface of the PEC. When the fields are discretized using the Yee method, continuity of the normal component of magnetic induction **B** across this interface is automatically satisfied, as these components are calculated using values of $\mathbf{E}_{tan}$ on the surface.

Weidelt code

An analytic solution for the quasi-static impulse response of a perfectly conducting half-plane in a conducting host was programmed, as derived by Weidelt (1999). This solution is also discussed in Appendix C of Johnson (1997). The half-plane model can be used to simulate the EM response obtained near the edge of a large platelike body of massive sulfide mineralisation, as found in the Sudbury basin and Kambalda nickel provinces. It is also a useful 2.5-D model for use in validating the model responses calculated using the FDTD codes and was used to verify that the electromagnetic responses of perfectly conducting bodies can be accurately estimated using the FDTD method.

CODE VALIDATION TESTS

Weidelt half-plane solution versus WH FDTD

The model used to verify the WH FDTD code by comparing it with the Weidelt code is shown in Figure 1 . It consists of a perfectly conducting half-plane lying within a medium with conductivity of 0.001 S/m. The magnetic dipole transmitter is

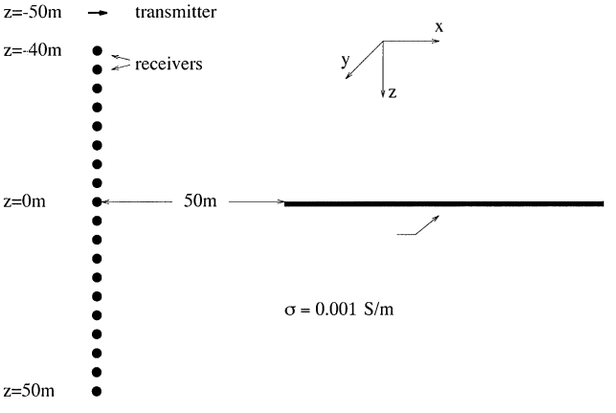

FIG. 1. Cross-section of the PEC half-plane model. The conductor extends infinitely to the right and perpendicular to the page.

oriented in the horizontal direction perpendicular to the edge, and placed 50 m above and to the left of the half-plane, in order to achieve good coupling to the target. The time domain waveform of the transmitter consists of a unit magnetic moment. A series of receivers measuring the vertical magnetic field are placed below the transmitter, recording the time derivative of the magnetic field intensity (i.e., the impulse response).

The perfectly conducting half-plane is incorporated in the FDTD model by explicitly setting the electric field components to zero at nodes lying within the half-plane before updating the magnetic field at each time step. The numerical response obtained using a cell size of 1 m within the region of interest agrees well with the closed-form result, particularly at late times (Figure 2). The z component of the magnetic field response is used in this comparison because the whole-space contribution is equal to zero for this set of receivers, giving a response that is entirely due to the half-plane. The discrepancy between the analytic and numerical responses decreases with increasing resolution. These results give us confidence that the analytic result is correct and that the quasi-static impulse response of a perfectly conducting half-plane can be accurately computed using the FDTD approach.

Validation of FJ FDTD code

The Yee algorithm has been exhaustively tested for models involving scattering from perfectly conducting objects in the wave-propagation regime. A survey of the relevant literature is provided by Shlager and Schneider (1995). The Furse code that was adapted by Johnson for geophysical applications has been tested against analytical and measured values in the megahertz and gigahertz range (Furse et al., 1990, 1997; Lazzi et al., 1998) and at 60 Hz (Furse and Gandhi, 1998). Its performance is examined in the FJ implementation for scattering in the diffusion regime. The strategy is thus to rigorously test the code for both end regimes as a necessary condition for correctness for all frequency regimes.

The full-wave FJ code is used to simulate the response of a perfectly conducting plate measuring 200 m in length and 150 m in width (Figure 3) within a medium with conductivity 0.001 S/m. The finite difference mesh consists of $100 \times 150 \times 150$ cubic cells of dimension $\Delta x = 2$ m. A y-directed magnetic dipole transmitter is placed 100 m above the surface of the plate and 50 m from its edge, with a vertical line of receivers placed below the transmitter. The transmitter time-domain waveform consists of a Gaussian pulse with an amplitude spectrum decreasing to half of its peak value at 300 kHz. The analogous half-plane model response is also calculated by convolving the closed-form impulse response solution with the transmitter waveform used in the FDTD simulation. The host resistivity and transmitter frequency range of the model are chosen so that the quasi-static assumption is valid.

Comparison of the vertical magnetic field responses (Figure 4) for the receiver opposite the edge of the plate suggests that the finite-dimensional plate is an imperfect representation

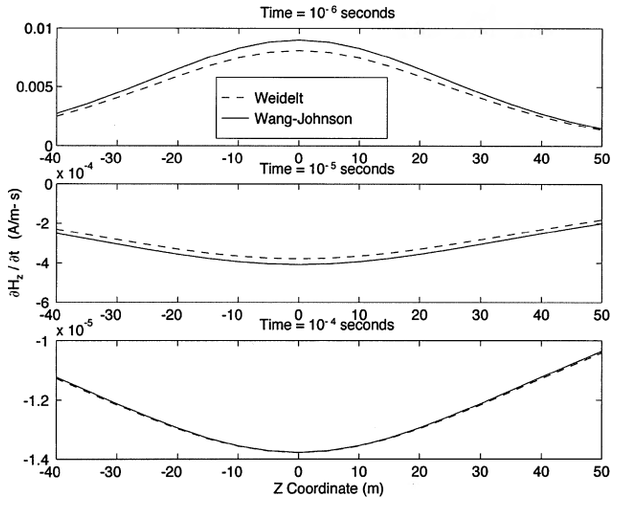

FIG. 2. Comparison of the analytic result for a perfectly conducting half-plane due to Weidelt (1999) with the numerical solution obtained using the FDTD algorithm of Wang and Hohmann (1993) with PEC boundary conditions enforced explicitly at each time step. The calculated impulse responses are compared at delay times of 10^{-6}, 10^{-5}, and 10^{-4} s.

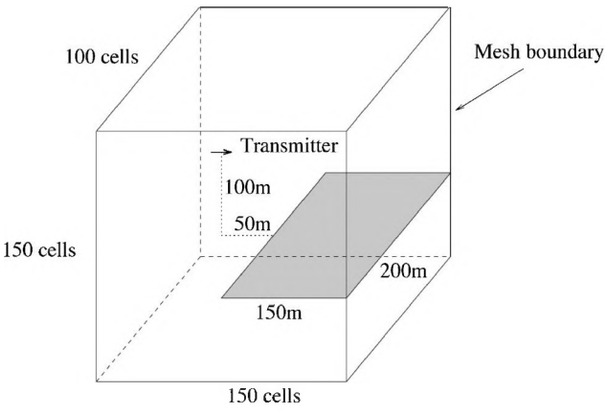

FIG. 3. Plate model used to represent a perfectly conducting half-plane.

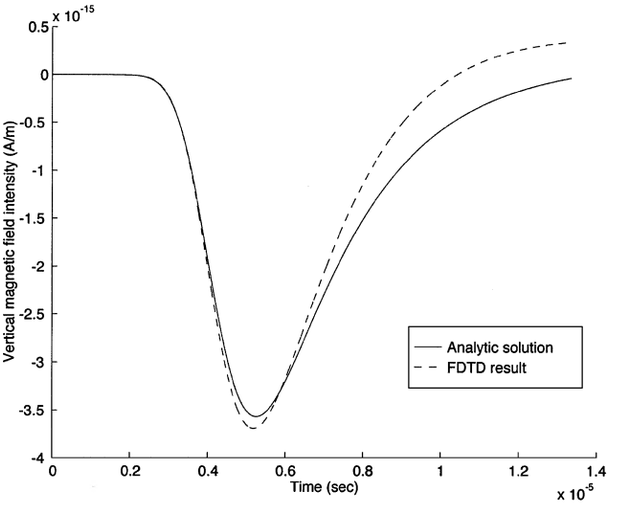

FIG. 4. Comparison of the vertical magnetic field response of the model depicted in Figure 3 with the analytic solution for the analogous half-plane model.

of an infinite half-plane. Hanneson (1981) found that, for a horizontal-loop EM prospecting system with a loop separation L, a thin vertical plate can be considered effectively infinite when its length is $\geq 3L$ and its width $\geq 1.5L$. Using this criterion, a transmitter-receiver separation of 100 m would require a plate of length 300 m and width 150 m for the simulation of a half-plane response. Unlike the WH code, which models the fields within a large volume with cells of increasing size, the FJ code uses a uniform mesh to model a restricted region, so that the dimensions of the plate that can be modeled using the FJ code are considerably smaller than those of the plate simulated by the WH code. This is a limitation of the FJ code, rather than the algorithm itself. The response of the plate modeled using the FJ algorithm decays more rapidly at late times than the response of the true half-plane. However, since early time and peak scattered field values for the two models are in good agreement, it is assumed that the FDTD fields for a physically larger plate would provide a better match to the analytical half-plane response. Hence, we tentatively conclude that the Yee algorithm can be used to accurately estimate the response of a perfectly conducting body in the diffusion regime.

Comparison of WH, FJ, and WT codes

In summary, the WH code provides an efficient and accurate means of calculating the quasi-static impulse response of a perfectly conducting body. The WT and FJ codes can be used to calculate full-wave EM responses, and our numerical experiments suggest that the FJ code can accurately model PEC responses in the quasi-static regime as well as at higher frequencies. Since the FJ code has been validated for free-space EM scattering from PEC targets, the necessary conditions for accuracy in the transitional frequency range have been established. The WT algorithm has superior numerical dispersion characteristics (Wang and Tripp, 1996), but the Liao absorbing boundary conditions used in the WT code depend upon the establishment of a sufficiently large separation between the mesh boundaries and any transmitters, scatterers or receivers placed therein.

Further details concerning code development are contained in Johnson (1997) and Johnson et al. (1998).

EXPERIMENTS IN SURVEY DESIGN

The ability of geophysical measurements to resolve geological features is limited by such factors as noise and the physical parameters of the survey and geology. We can usually control only the survey design, subject to physical access restrictions and the limitations of our instruments. Therefore, it is important to design the survey in a manner that maximizes the sensitivity of measurements to the geological parameters of interest. In order to determine the parameter sensitivities accurately, we might perform a rigorous sensitivity analysis based on singular value decomposition, which maps data uncertainties into parameter uncertainties (Kriesghäuser et al., 1996). However, we can also perform simple forward modeling experiments to estimate ideal noise-free sensitivities for measurements taken within a given region, which indicate where data must be measured in order to obtain optimal resolution under ideal conditions. In this case, we compare the data generated by one model with those generated by a similar model in which the parameters of interest have been perturbed. In performing the actual survey, we should collect the measurements that are most sensitive to perturbations in the parameters of interest. Whether or not these measurements are sufficiently sensitive for the parameters to be resolved to the desired level of accuracy is a question that can only be answered with reference to the predicted noise model and the instrument specifications.

Forward modeling of the thin plate model

Consider the case where a platelike body of massive sulfide mineralization has been intersected by several drill holes. The lateral position of the body is known, and it is desired to determine its vertical extent for the purposes of ore reserve calculation and mine planning. It is possible to determine the depth extent by drilling more holes, although it may be more cost-effective to use geophysical methods. A cross-borehole electromagnetic survey can be carried out using a magnetic dipole transmitter operating at several different frequencies. For a given transmitter location, it is desired to determine the receiver positions that will be most sensitive to the plate edge.

We use the FJ code to calculate the electromagnetic fields at 300 kHz, 500 kHz, 1 MHz, and 2 MHz for two perfectly conducting plate models in which the position of the upper plate edge differs by 30 m (Figure 5). In both cases, a horizontal magnetic dipole transmitter is placed at the position $(x, z) = (30\text{ m}, 90\text{ m})$, the conductivity of the host rock is 0.001 S/m, and the electric permittivity is $6.4\,\varepsilon_0$. The fields are recorded in a vertical plane perpendicular to the plates and containing the transmitter. The plates extend 50 m to either side of the survey plane. The model in which the upper edges of the plate lies at $z = 90$ m is denoted as B. The other model is denoted as A.

A conventional radio imaging method (RIM) survey collects only amplitude data that are usually expressed in decibels relative to some arbitrarily chosen signal level. Therefore, it is useful to examine the model amplitude responses and sensitivities. For the purposes of visualization, the amplitude data are

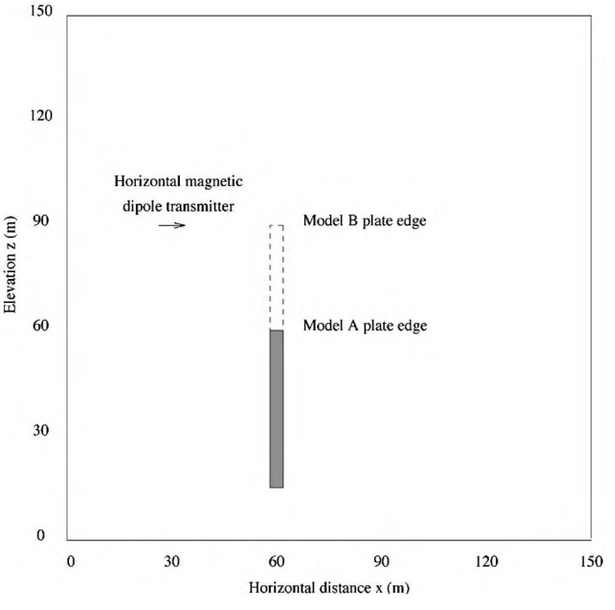

FIG. 5. Perfectly conducting plate models.

transformed as

$$F' = 20 \log \frac{F}{F_{\max}}, \tag{2}$$

where F is the field amplitude and $F_{\max}$ is the maximum value. The values of the transformed field F' are clipped at a lower bound of $F' = -500$ dB. This transformation, although somewhat arbitrary, facilitates image display.

The transformed amplitudes of the horizontal magnetic field components H_x at 2 MHz for model B (Figure 6) display a distinct shadow zone behind the plate, particularly in the lower portion of the target. Electromagnetic waves are diffracted by the edges of the plate, creating a zone of partial shadow behind the upper portion of the plate.

Two sets of model data are used to calculate the sensitivity of the measurements to the position of the plate's upper edge. The observed field can be expressed as a sum of a primary field component due to the dipole in a homogeneous whole-space and a secondary field component due to scattering from the target. Since we want to examine the difference in response between two models, it is useful to express the field perturbation due to the change in the plate edge position in decibels relative to the unperturbed model fields, so that

$$F = 20 \log \left| \frac{F^A - F^B}{F^A + \varepsilon} \right|, \tag{3}$$

where F^A and F^B are the amplitude responses of the unperturbed model A and the perturbed model B, respectively, and ε is a small number chosen to prevent F from becoming undefined when $F^A = 0$.

For an instrument of given dynamic range and an estimated level of observational error, we can use maps of F to decide whether a given measurement is likely to yield useful information regarding the vertical extent of the plate. The map of F at 2 MHz (Figure 7) indicates that the data that best resolve the position of the plate lie within a wedge-shaped zone radiating from the top edge of the plate in model B and lying on the far side of the plate relative to the transmitter. If the transmitter frequency is lowered to 500 kHz (Figure 8), then the zone of maximum sensitivity only extends about 30 m horizontally from the plate, unlike the case at 2 MHz. The required sensitivity threshold of the instrument decreases more rapidly with distance from the target, and optimal positioning of receivers becomes more important as the frequency is lowered.

Replacing the 2-MHz horizontal magnetic-field transmitter with a vertical magnetic dipole and measuring the vertical magnetic field component results in a marked change in the sensitivity map (Figure 9). The area enclosed by the −10 dB sensitivity contour is now greater than the area enclosed for the horizontal transmitters and receivers (compare with Figure 7).

Now consider an instance where a part of the original orebody has been displaced by faulting, and we wish to determine a survey design that will allow us to resolve this feature. Using the FJ code, the responses of two models were computed: one in which a plate of 75 m vertical extent is excited by a vertical magnetic dipole, and another in which the top 30 m of the plate is displaced horizontally 20 m away from the transmitter (Figure 10). As in the previous example, the width of the plate is 100 m.

Amplitude data are modeled at 2 MHz and 500 kHz, and the sensitivities in a vertical slice containing the transmitter are calculated as in the previous example. For a transmitter frequency of 2 MHz, the data behind the lower portion of the ore body can

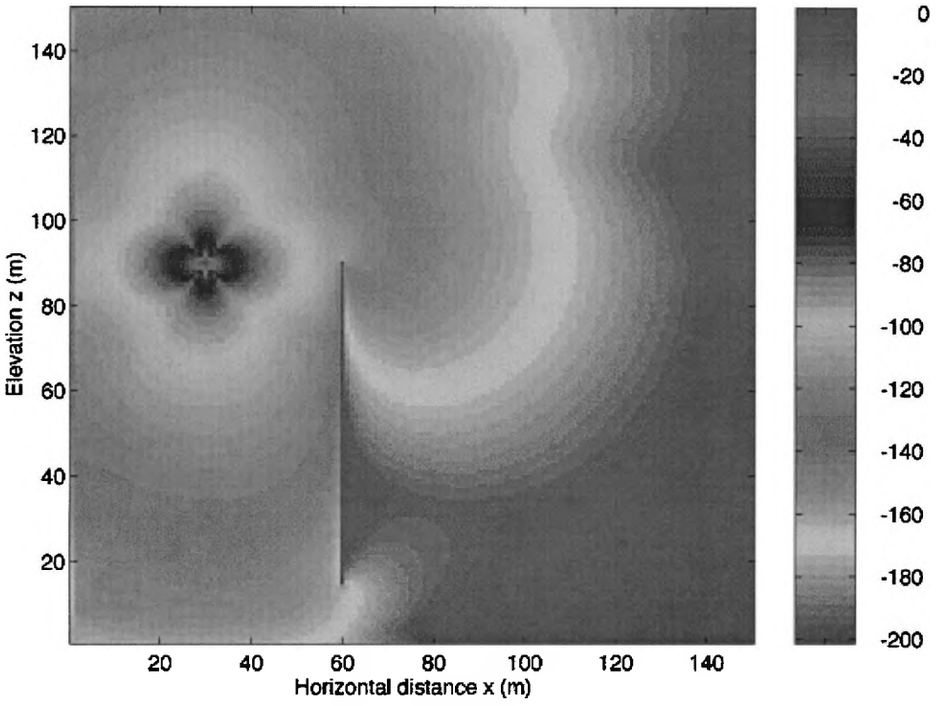

FIG. 6. Horizontal magnetic field amplitudes for model B at 2 MHz expressed in decibels relative to the maximum value. The minimum has been clipped at −500 dB.

be used to resolve the throw of the fault (Figure 11), whereas the data acquired at 500 kHz are comparatively insensitive to the offset (Figure 12). The lateral resolution of the survey deteriorates rapidly with decreasing frequency.

Confidence limits of parameter resolution

Sensitivities of data to perturbations in a model parameter (i.e., Frechet derivatives) can be plotted as a function of measurement location in order to determine the locations where

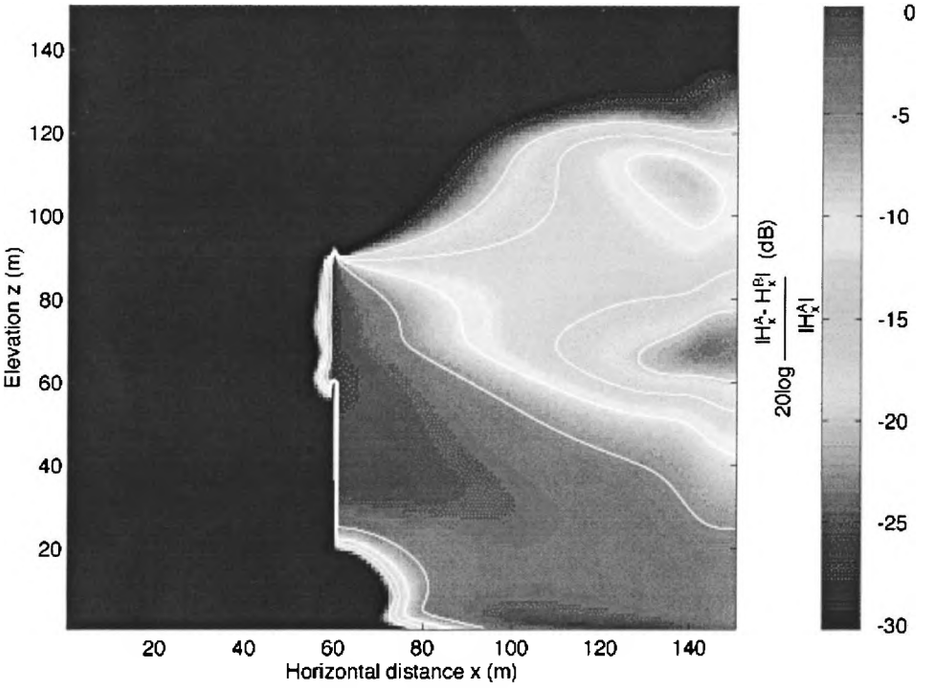

FIG. 7. Horizontal magnetic-field amplitude perturbations in decibels relative to the unperturbed model response at 2 MHz, where the minimum has been clipped at −30 dB. Contours at −5, −10, −15, and −20 dB are shown.

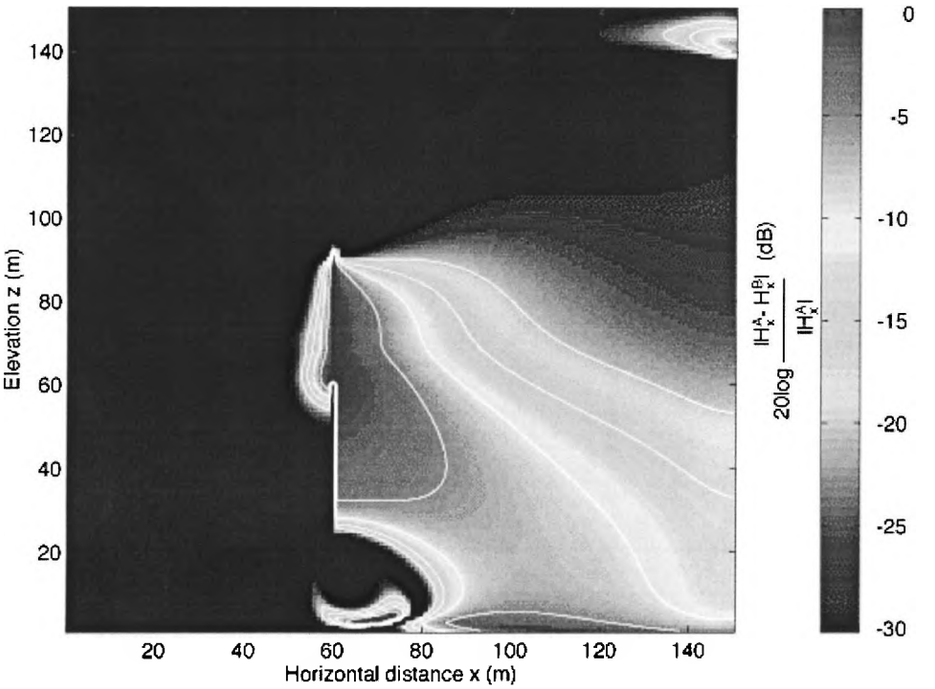

FIG. 8. Horizontal magnetic-field amplitude perturbations in decibels relative to the unperturbed model response at 500 kHz, where the minimum has been clipped at −30 dB. Contours at −5, −10, and −20 dB are shown.

the data are most sensitive to the model parameter of interest. However, these maps are of limited usefulness insofar as they do not consider measurement error. If a certain amount of noise is introduced, then the degree to which each datum can be used to resolve a parameter depends upon the magnitude of that datum relative to the error, as well as the magnitude of the Frechet derivative. We then require a means of mapping data errors into parameter uncertainties.

Assuming that perturbations in data are linearly related to perturbations in model parameters through the Jacobian matrix, we can use the singular value decomposition (SVD) of the Jacobian to estimate the parameter covariance matrix **C** from the data standard errors (Martin, 1971). For a model containing v free parameters, confidence intervals for each parameter p_j are given by

$$\delta p_j = \pm\sqrt{\frac{\Delta\chi_v^2}{C_{jj}}} \tag{4}$$

(Press et al., 1992, 690–691), where $\Delta\chi_v^2$ is the χ^2 variable of v degrees of freedom for the desired confidence levels. Using these estimates of the parameter uncertainties, we can evaluate the usefulness of data acquired at different locations in resolving a given parameter. An application of this method to cross-borehole EM survey design is discussed below.

Cross-borehole EM surveys usually consist of measurements taken at a number of receiver locations, using several different transmitter deployments. This is done to record data for several different illuminations of the target. We need to determine the locations at which we should place receivers in order to achieve optimal resolution of a parameter of interest. Consider the case where two boreholes have been drilled on either side of a large sheet of highly conductive sulfide mineralization (Figure 13). The position of the sheet edge is to be determined using cross-borehole electromagnetic data. Model data were generated using the quasi-static analytic solution for the PEC half-plane (Weidelt, 1999) because of its computational efficiency. Two

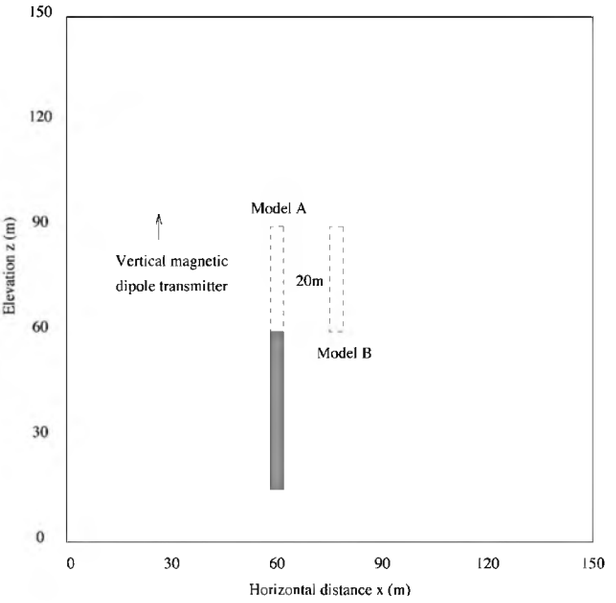

FIG. 10. Faulted and intact perfectly conducting plate models. The dashed line shows the position of the upper 30 m of the orebody in each case. The dipole transmitter lies opposite the top edge of the orebody.

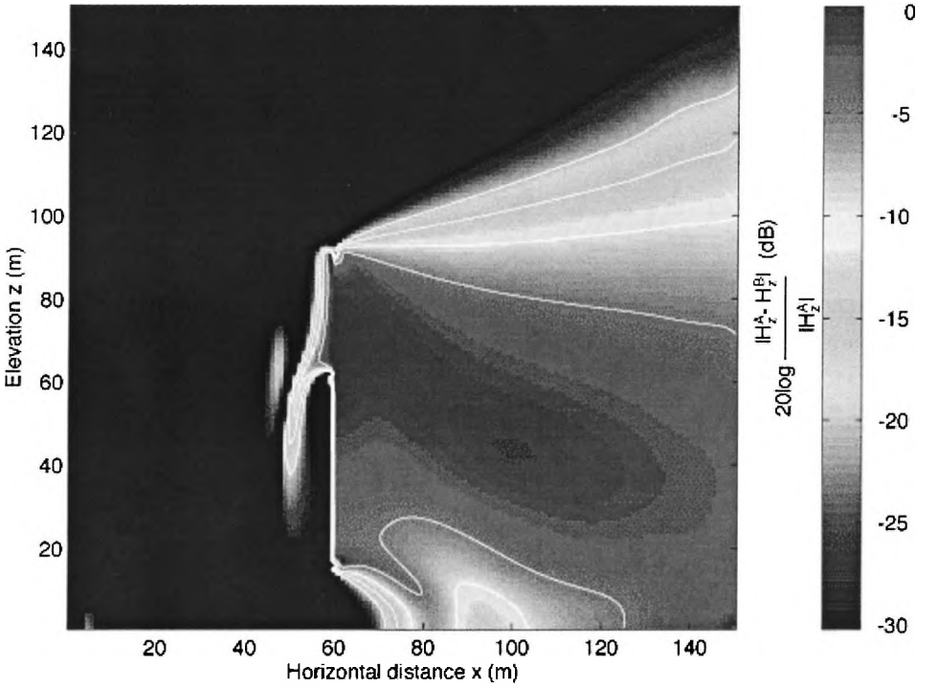

FIG. 9. Vertical magnetic-field amplitude perturbations in decibels relative to the unperturbed model response at 2 MHz, where the minimum has been clipped at −30 dB. Contours at −5, −10, −15, and −20 dB are shown.

cases were considered, in which the position of the half-plane edge differs by 20 m vertically (Figure 14). The conductivity of the host material is 0.001 S/m. In each case, an array of receivers with a spacing of 5 m is placed in one borehole. Magnetic field responses are calculated for a vertical magnetic dipole (VMD) transmitter operating at 300 kHz and placed in turn at 5-m spaced positions in the other borehole. These models emulate the tomographic mode of cross-borehole EM surveying in

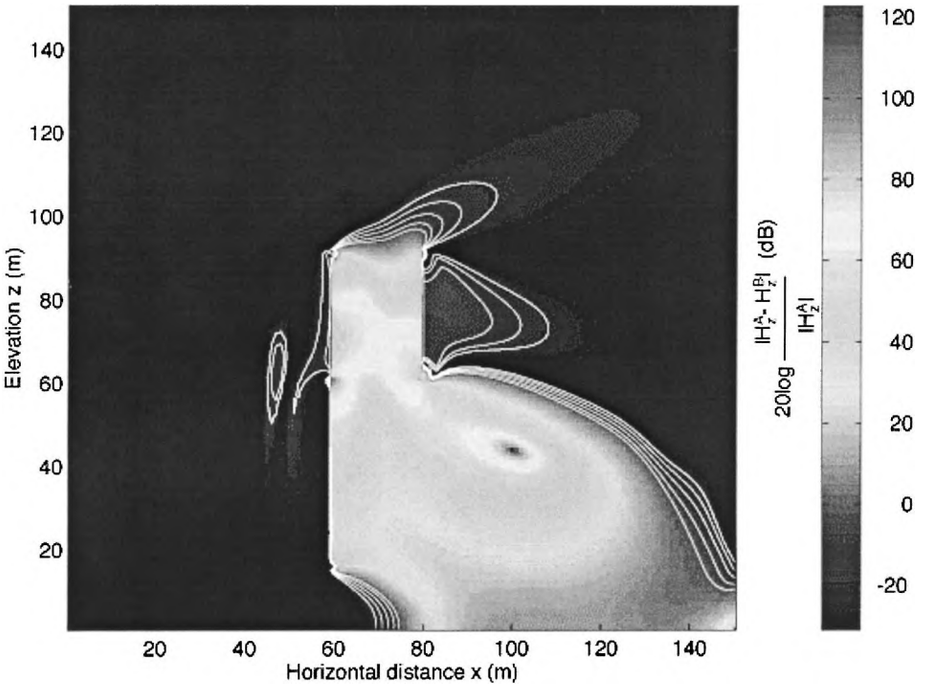

FIG. 11. Vertical magnetic-field amplitude perturbations in decibels relative to the unperturbed model response at 2 MHz, where the minimum has been clipped at −30 dB. Contours at −1, −5, −10, −15, and −20 dB are shown.

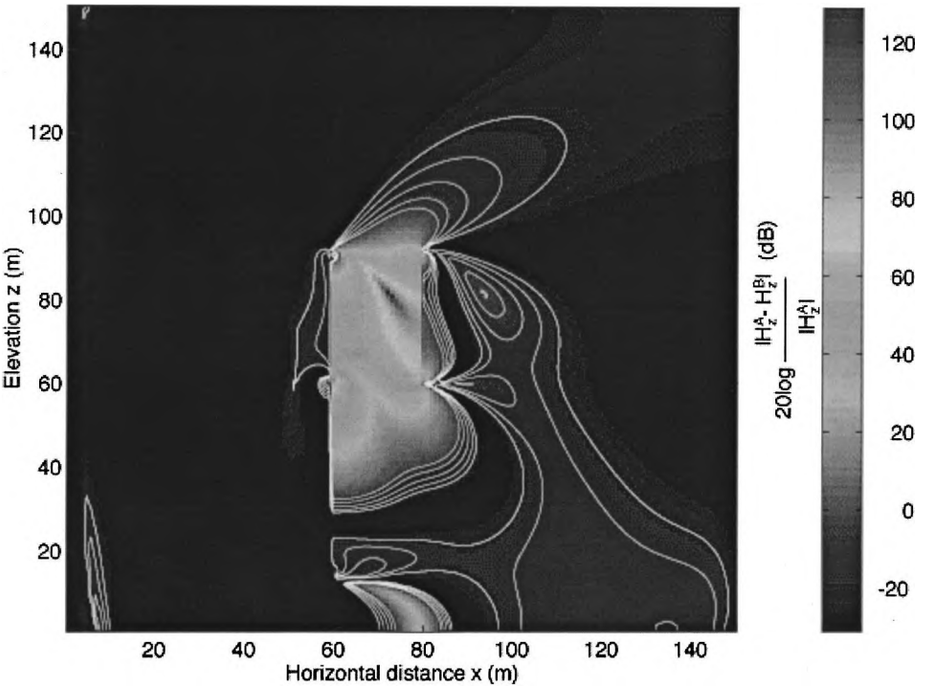

FIG. 12. Vertical magnetic field amplitude perturbations in decibels relative to the unperturbed model response at 500 kHz, where the minimum has been clipped at −30 dB. Contours at −1, −5, −10, −15, and −20 dB are shown.

common use. Frechet derivatives are estimated by differencing the model results. For each receiver location, a Jacobian matrix is formed from the sensitivities corresponding to the transmitter array.

Assuming standard errors of 10% and 20% for each measurement, the 99% confidence intervals for the position of the half-plane edge are estimated for each receiver location using the method described above (Figure 15). This mapping of data errors onto parameter uncertainties shows that receivers placed well above the sheet edge do not record data that can be used to closely constrain our estimate of its position. It is obvious that data must be recorded at positions below the edge of the half-plane. Parameter uncertainties corresponding to receivers within the "shadow zone" of the plate are fairly uniform, increasing slightly as the signal magnitude decreases with depth.

If both the vertical and lateral positions of the half-plane edge must be estimated from the data, then the parameter uncertainties are expected to be somewhat greater. Allowing both parameters to vary, and assuming uniform standard errors of 10%, 15%, and 20% for each measurement, the 99% confidence intervals for the vertical and lateral positions of the edge were estimated (Figure 16) using the method described above. Our ability to resolve the vertical position of the conductor edge decreases for all receiver positions, and optimal positioning of the measurements becomes more critical (compare Figures 15 and 16a). Estimates of the lateral position of the conductor (Figure 16b) have higher uncertainties by a factor of about two over all. Both vertical and lateral resolutions

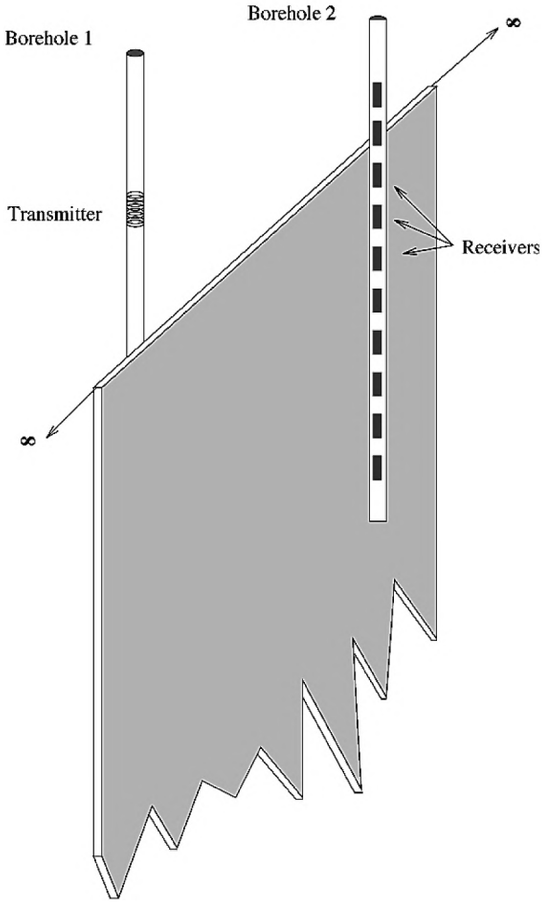

FIG. 13. Perfectly conducting vertical half-plane lying between two vertical boreholes. An array of vertical magnetic dipole (VMD) transmitters is placed in borehole 1, and an array of magnetic-field receivers is placed in borehole 2. The half-plane extends to infinity downward and perpendicular to the plane containing the boreholes.

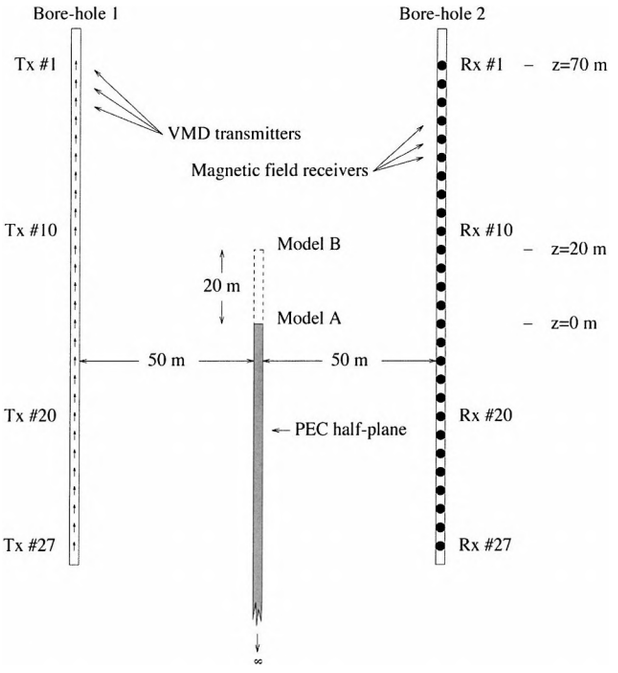

FIG. 14. Schematic diagram showing two half-plane models in which the vertical position of the edge is perturbed by 20 m.

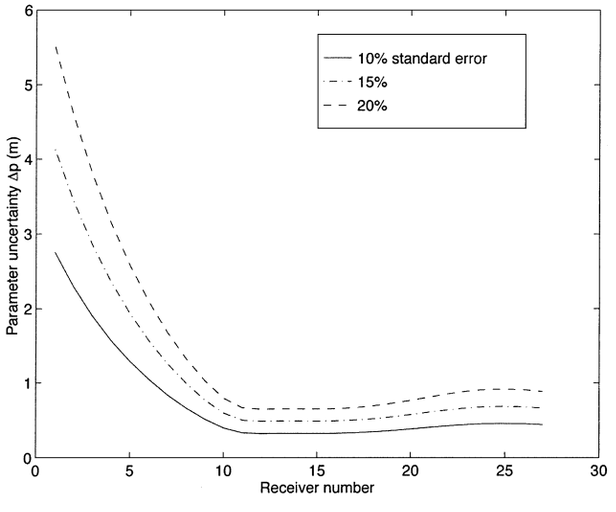

FIG. 15. Estimated uncertainties for the height of the half-plane edge within the 99% confidence region, given uniform data standard errors of 10%, 15%, and 20%. The parameter is estimated using data recorded at each receiver for the set of 27 transmitters, and the uncertainty is plotted for each receiver number.

are optimal for the receiver lying at the same height as the edge of the half-plane in the unperturbed model. In designing a survey to estimate the vertical and lateral position of the conductor to within a few meters, we should plan to measure data within the range of depths where the edge of the conductor is expected to lie. Data measured above the conductor have very poor sensitivity to the parameters of interest, especially in the presence of noise. The slight increase in parameter uncertainty estimates at depths below the plate edge is more marked in this case than it was when only the vertical position was allowed to vary (compare Figures 15 and 16). The deleterious effect of noise upon resolution becomes more acute as the number of parameters to be estimated increases.

There are two main problems with this method of estimating uncertainties, that both lead to estimates of the parameter uncertainties that are unrealistically small. First, it relies on the assumption that the mappings between perturbations in data and parameters are linear. In electromagnetic models, this assumption usually holds only over a small range of parameter variations. Second, the use of uniform data relative errors implies that we can measure signals over an arbitrary dynamic range to that level of accuracy. In practice, geophysical instruments have a limited dynamic range.

Optimization of transmitter arrays

Cherkaeva and Tripp (1996) have shown that given sufficient a priori information concerning the geological setting of a geoelectric survey, it is possible to find an applied current distribution that maximizes the sensitivity of measurements to a geologic feature of interest. The method derived by these authors is briefly outlined below, with particular application to the cross-borehole EM problem. A simple but practical example is used to illustrate the method.

Consider a set of electromagnetic measurements taken in the vicinity of an array of dipole transmitters and a given distribution of physical properties denoted as σ. Let each transmitter have a moment of magnitude w_I, so that

$$F^{\sigma}\mathbf{w} = \mathbf{d}, \tag{5}$$

where F^{σ} is an operator that maps the vector of transmitter weights $\mathbf{w} = [w_1, w_2, w_3 \ldots w_N]$ onto the vector of data $\mathbf{d}$. We can also consider the measured data as a weighted sum of responses to a set of unit dipoles placed at each transmitter location, with $\mathbf{w}$ as the set of weights.

If the distribution of physical properties is perturbed, then we can write an operator equation for the perturbed geophysical model denoted as $\sigma + \delta$:

$$F^{\sigma+\delta}\mathbf{w} = \mathbf{d}^{\delta}, \tag{6}$$

where $F^{\sigma+\delta}$ is the perturbed operator which maps the vector of moments $\mathbf{w}$ onto the perturbed data $\mathbf{d}^{\delta}$.

One measure of the sensitivity of the measured data to the perturbation is the L_2 norm of the data residual $\mathbf{d} - \mathbf{d}^{\delta}$. We denote this quantity as I^2, which can be considered a measure of the information content of the data with respect to the perturbed model parameter. Thus we write,

$$I^2 = \|(F^{\sigma+\delta} - F^{\sigma})\mathbf{w}\|^2. \tag{7}$$

We would like to find the set of moments $\mathbf{w}$ that maximizes the magnitude of I. The measured response scales with $\mathbf{w}$, and we wish to find the geometry of the optimal transmitter moments, so we optimize I subject to $\|\mathbf{w}\|^2 = 1$, where

$$M_1 = \max I(\mathbf{w}) = \max \|(F^{\sigma+\delta} - F^{\sigma})\mathbf{w}\|, \quad \mathbf{w} : \|\mathbf{w}\|^2 = 1. \tag{8}$$

This is an eigenvalue problem, wherein the optimal set of transmitter moments $\mathbf{w}$ is the eigenvector corresponding to the maximum eigenvalue M_1. An example of how this technique might be applied to optimization of cross-borehole EM survey resolution is discussed below.

Consider the problem of detecting the edge of a conductive sheet discussed previously. We will again use the Weidelt code to generate the model data. Data are recorded at each receiver location using a number of different transmitters (Figure 14). It is possible to form a weighted sum of the data recorded at each receiver location that has optimal sensitivity to the parameter of interest. Considering only amplitude data, the optimal weights for this transmitter array are estimated using the SVD of the impedance matrix, and the sensitivities of the resulting data are compared with the sensitivities corresponding to a uniform weighting (Figure 17). The maximum sensitivity is improved by about 20% by using optimal weightings, as opposed to a uniform weighting.

The optimized weightings have the effect of emphasizing those transmitters for which the measured data have the greatest sensitivity to the model parameter of interest. Conversely, data that are unimportant are deemphasized, so that there is less opportunity for errors in these measurements to contribute uncertainty to the estimation of the model parameter. Thus, the distribution of weightings shown in Figure 17b has a shape similar to that of the optimal sensitivity distribution shown in Figure 17a. Accuracy of the survey can clearly be improved by preanalyzing the receiver sensitivity to model perturbations and weighting them accordingly.

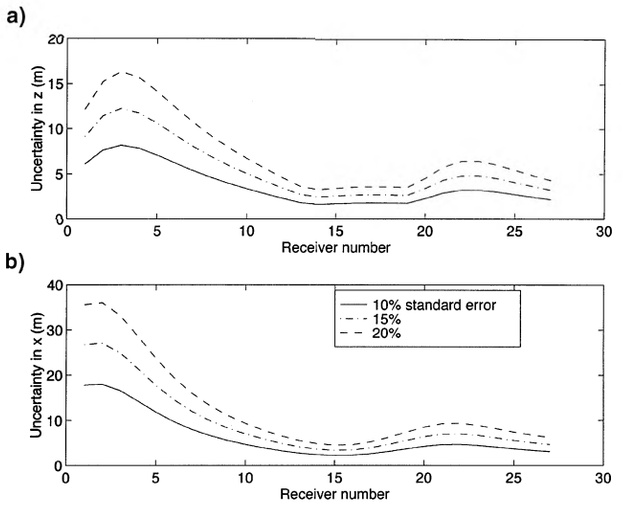

FIG. 16. Estimated uncertainties for the position of the half-plane edge within the 99% confidence region, given uniform data standard errors of 10, 15, and 20%: (a) uncertainties for the vertical position, (b) uncertainties for the lateral position.

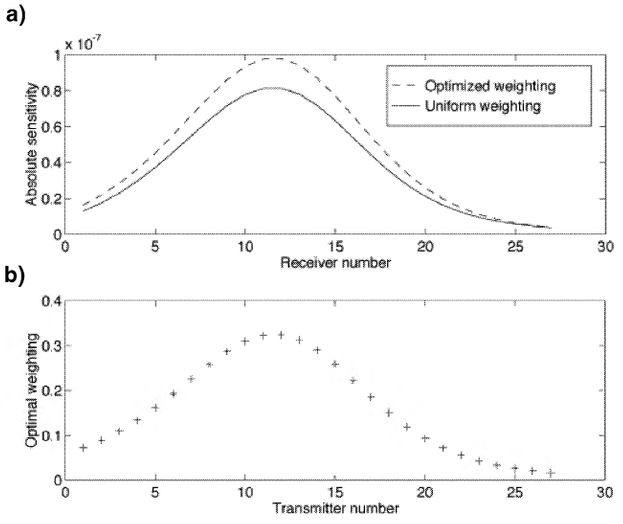

FIG. 17. Optimization of sensitivities for a weighted transmitter array: (a) sensitivities of data for the uniformly and optimally weighted transmitter arrays, (b) the set of optimal weights applied to each transmitter. The model geometry is shown in Figure 14.

CONCLUSIONS

Four codes were compared for analysis of cross-borehole surveys of electromagnetic exploration for nickel sulfide deposits using frequencies from 500 kHz to 2 MHz. The Wang-Hohmann FDTD code was shown to be an accurate assessment tool in the quasi-static regime. The Furse-Johnson traditional FDTD code was shown to be an accurate tool for both quasi-static and higher frequency regimes. The Wang-Tripp code was evaluated but not used for these simulations because of inaccuracies of the boundary conditions in this code near the quasi-static regime. The analytical solution by Weidelt was shown to be accurate and useful for simple plate geometries.

These codes were used to evaluate thin plates of highly conductive ore (modeled as perfect electric conductors) in faulted and unfaulted conditions, and the diffractive nature of the fields was observed. The perturbation of the fields from different ore configurations was mapped, showing that there are distinct triangular-shaped regions of maximum sensitivity (maximum field perturbation) where receivers should be placed behind the orebodies. These regions were found to be larger for higher frequencies, showing that better resolution modeling is possible with the higher frequencies despite reduced power deposition at higher frequencies. Using these maps of receiver sensitivity, weightings for each receiver were optimized in order to maximize the confidence levels on the size and shape of the orebody.

ACKNOWLEDGMENTS

David Johnson thanks the Consortium for Electromagnetic Modeling and Inversion for financial support. Alan Trip and Elena Cherkaev thank the Department of Energy under contract no. DE-FG03-93ER14313 for financial support. The assistance of P. Weidelt with analytical plate solution is gratefully acknowledged.

REFERENCES

Annan, A. P., 1974, The equivalent source method for electromagnetic scattering analysis and its geophysical application: Ph.D. thesis, Memorial Univ. of Newfoundland.
Berenger, J.-P., 1994, A perfectly matched layer for the absorption of electromagnetic waves: J. Comput. Phys., **114**, 185–200.
Chen, Y. H., Chew, W. C., and Oristaglio, M. L., 1996, Transient modeling of subsurface EM problems using PML ABC: 66th Ann. Internat. Mtg., Soc. Expl. Geophys., Expanded Abstracts, 245–248.
Cherkaeva, E., and Tripp, A. C., 1996, Optimal survey design using focused resistivity arrays: IEEE Trans. Geosci. Remote Sensing, **34**, 358–366.
Chew, W. C., 1990, Waves and fields in inhomogeneous media: Van Nostrand Reinhold.
Chew, W. C., and Weedon, W. H., 1994, A 3-D perfectly matched medium for modified Maxwell's equations with stretched coordinates: Micro. Opt. Tech. Lett., **7**, 599–604.
Fang, J., and Wu, Z., 1995, Generalized perfectly matched layer—An extension of Berenger's perfectly matched layer boundary condition: IEEE Micro and Guided Lett., **5**, 451–453.
Fullagar, P. K., and Livelybrooks, D., 1994, Trial of tunnel radar for cavity and ore detection in the Sudbury mining camp, Ontario: 5th Internat. Conf. on Ground Penetrating Radar, Proceedings, **3**, 883–894.
Furse, C. M., and Gandhi, O. P., 1998, Calculation of electric fields and currents induced in a millimeter-resolution human model at 60 Hz using the FDTD method: Bioelectromagnetics, **19**, 293–299.
Furse, C. M., Mathur, S. P., and Gandhi, O. P., 1990, Improvements to the finite-difference time-domain method for calculating radar cross section of a perfectly conducting target: IEEE Trans. Microwave Theory and Techniques, **38**, 919–927.
Furse, C. M., Yu, Q. S., and Gandhi, O. P., 1997, Validation of the finite-difference time-domain method for near field bioelectromagnetic simulations: Microwave and Optical Technology Lett., 341–345
Gresham, J. J., and Loftus-Hills, G. D., 1981, The geology of the Kambalda nickel field, Western Australia: Econ. Geol., **76**, 1373–1416.
Hanneson, J. E., 1981, The horizontal loop EM response of a thin vertical conductor in a conducting half-space: Ph.D. thesis, Univ. of Manitoba.
Hohmann, G. W., 1983, Three-dimensional EM modeling: Geophys. Surv., **6**, 27–53.
Kriegshäuser, B., Tripp, A. C., and Tabarovsky, L., 1996, Experimental design for surface-to-borehole hydrocarbon applications: 66th Ann. Internat. Mtg., Soc. Expl. Geophys., Expanded Abstracts, 234–237.
Johnson, D. M., 1997, Finite difference time domain modeling of cross-hole electromagnetic survey data: M.Sc. thesis, Univ. of Utah.
Johnson, D. M., Furse, C., and Tripp, A. C., 1998, FDTD modeling of the electromagnetic response of a conductive ore deposit in a lossy dielectric: submitted to Geophysics.
Lazzi, G., Pattnaik, S. S., Furse, C. M., and Gandhi, O. P., 1998, Comparison of FDTD-computed and measured radiation patterns of commercial mobile telephones in presence of the human head: IEEE Trans. Antennas and Propagation, **46**, 943–944
Martin, B. R., 1971, Statistics for physicists: Academic Press Inc.
Mur, G., 1981, Absorbing boundary conditions for the finite-difference approximation of the time-domain electromagnetic field equations: IEEE Trans. Electromagn. Compat., **23**, 377–382.
Nickel, H., and Cerny, I., 1989, More effective underground exploration for ores using radio: Expl. Geophys., **20**, 371–377.
Pitts, B., and Kramers, A., 1996, The application of high resolution crosswell radio tomography in the exploration of base metal ore deposits: 66th Ann. Internat. Mtg., Soc. Expl. Geophys., Expanded Abstracts, 622–625.
Press, W. H., Teukolsky, S. A., Vetterling, W. T., and Flannery, B. P., 1992, Numerical recipes in FORTRAN: Cambridge Univ. Press.
Rao, V. M., and Rao, I. B. R., 1983, The radio absorption technique in Mailaram copper mines, India: Geophysics, **48**, 391–395.
San Filipo, W. A., Eaton, P. A., and Hohmann, G. W., 1985, Integral equation solution for the transient electromagnetic response of a three-dimensional body in a conductive half-space: Geophysics, **50**, 798–809.
Shlager, K. L., and Schneider, J. B., 1995, A selective survey of the finite-difference time-domain literature: IEEE Antennas and Propagation Magazine, **37**, no. 4, 39–56.
Stanton, R. L., 1972, Ore petrology: McGraw-Hill Book Co.
Stolarczyk, L. G., 1990, Radio imaging in seam guides, *in* Ward, S. H., Ed., Geotechnical and environmental geophysics, Soc. Expl. Geophys., 187–209.

——— 1992, Definition imaging of an orebody with the radio imaging method (RIM): IEEE Trans. Industry Applications, **28**, 1141–1147.

Stolarczyk, L. G., Rogers, G., and Hatherly, P., 1988, Comparison of radio imaging method (RIM-I) electromagnetic tomography with in-mine geological mapping in the Lidell, Bulli and Wongawilli coal seams: Expl. Geophys., **19**, 169–170.

Taflove, A., and Umashankar, K. R., 1989, The finite-difference time-domain method for numerical modeling of electromagnetic interactions with arbitrary structures, *in* Morgan, M.A., Ed., Progress in electromagnetics research, **2**, Elsevier Science Publ. Co., 287–333.

Thomson, S., Young, J., and Sheard, N., 1992, Base metal applications of the radio imaging method: Current status and case studies: Expl. Geophys., **23**, 367–372.

Wang, T., and Hohmann, G. W., 1993, A finite-difference time-domain solution for three-dimensional electromagnetic modeling: Geophysics, **58**, 797–809.

Wang, T., and Tripp, A. C., 1996, FDTD simulation of EM propagation in 3-D media: Geophysics, **61**, 110–120.

Wedepohl, E., 1993, Radio tomography: Imaging ore bodies using radios: 3rd Tech. Mtg., S. African Geophys. Assn., Expanded Abstracts, 95–99.

Weidelt, P. S., 1999, Transient electromagnetic edge diffraction as a simple test case for validating numerical 3D codes: presented at 2nd Internat. Symp. on 3DEM.

Yee, K. S., 1966, Numerical solution of initial boundary value problems involving Maxwell's equations in isotropic media: IEEE Trans. Antennas Prop, **14**, 302–307.